



NEXT GENERATION AUTOMOTIVE MEMBRANE ELECTRODE ASSEMBLIES

Grant agreement no.: 826097

Start date: 01.01.2019 – Duration: 42 months

Project Coordinator: Dr. Deborah Jones - CNRS

DELIVERABLE REPORT

| D6.4: POST-TEST ANALYSIS REPORT | | |
|--|---|----------|
| Due Date | 30.06.2022 | |
| Author (s) | Stefan Zink, Sylvain Brimaud, Ludwig Jörissen | |
| Workpackage | WP6 | |
| Workpackage Leader | ZSW | |
| Lead Beneficiary | ZSW | |
| Date released by WP leader | 25.07.2022 | |
| Date released by Coordinator | 26.07.2022 | |
| DISSEMINATION LEVEL | | |
| PU | Public | X |
| PP | Restricted to other programme participants (including the Commission Services) | |
| RE | Restricted to a group specified by the consortium (including the Commission Services) | |
| CO | Confidential, only for members of the consortium (including the Commission Services) | |
| NATURE OF THE DELIVERABLE | | |
| R | Report | X |
| P | Prototype | |
| D | Demonstrator | |
| O | Other | |

| SUMMARY | |
|-----------------|--|
| Keywords | <i>D6.4, post-test analysis</i> |
| Abstract | <i>The durability of the first two stack generations did not meet the GAIA durability target of less than 10 % degradation within 6000 operation hours sufficiently. For understanding the present degradation mechanisms, various post-test analyses were performed. Based on the achieved knowledge, the materials for the following stack generations were optimised accordingly to reach the GAIA durability target. A low membrane and ionomer stability at the given operating parameters at high loads of 3 A/cm² and high temperature of 105 °C were found to be the key points for the occurred degradation and addressed by material changes for the final stack generations.</i> |

| REVISIONS | | | |
|------------------|-------------|-------------------|----------------------|
| Version | Date | Changed by | Comments |
| 0.1 | 31.07.2022 | Stefan Zink | Drafted, final draft |
| 2.0 | 24.08.2022 | Stefan Zink | Revision |



This project has received funding from the Fuel Cells and Hydrogen 2 Joint Undertaking (now Clean Hydrogen Partnership) under grant agreement n°826097. This Joint Undertaking receives support from the European Union's Horizon 2020 Research and Innovation program, Hydrogen Europe and Hydrogen Europe Research.



D6.4 - POST-TEST ANALYSIS REPORT

CONTENTS

| | |
|-------------------------------------|----|
| 1. Introduction..... | 4 |
| 2. Scope | 4 |
| 3. Results and discussion | 6 |
| 4. Conclusions and future work..... | 14 |

1. INTRODUCTION

Besides good performance, the durability of a membrane electrode assembly (MEA) is crucial for its use in fuel cell stacks for automotive application. Therefore, in addition to the GAIA beginning of life (BoL) performance target of 1.8 W/cm² at 0.6 V, a durability of the GAIA MEA of 6000 operating hours with degradation of less than 10 % of the BoL cell voltage was the target. This durability target should be demonstrated by operating the GAIA MEA within a 10-cells short stack using the INSPIRE full size automotive stack hardware. For testing, a degradation drive cycle was developed by BMW at the beginning of the project (described in D2.3) based on real life data from the BMW car fleet. Thereby, the operation up to high current density of 3 A/cm² and the operation at a rather high temperature for PEMFC of 105 °C at the stack outlet were the most challenging targets. To determine the overall degradation, the short stack was operated using the drive cycle profile for 1000 operating hours, which was extrapolated to 6000 operating hours afterwards. Since the observed long-term stability of the Gen 1 MEA was not sufficient to meet the GAIA durability target at GAIA operating conditions, extensive post-mortem analyses were performed to understand the degradation mechanisms that occurred in order to tailor the future GAIA MEAs towards better long-term stability at the desired test conditions.

2. SCOPE

The generation 1 (Gen 1) stack containing state-of-the-art material from the INSPIRE project was used to set a benchmark for the GAIA project in terms of performance and durability at GAIA conditions. The main targets of GAIA are the operation of a fuel cells stack up to high current density of 3 A/cm² and an increased stack outlet temperature of 105 °C. Therefore, a tailored fuel cell test drive cycle was developed by BMW at the beginning of the project (Deliverable D2.3) based on real car driving behaviour (Figure 1). The observed voltage decay over time at the different operating points demonstrated decay rates clearly above the desired 12-14 μV/h, which is considered necessary to reach the GAIA durability target of less than 10 % voltage degradation within 6000 operation hours.

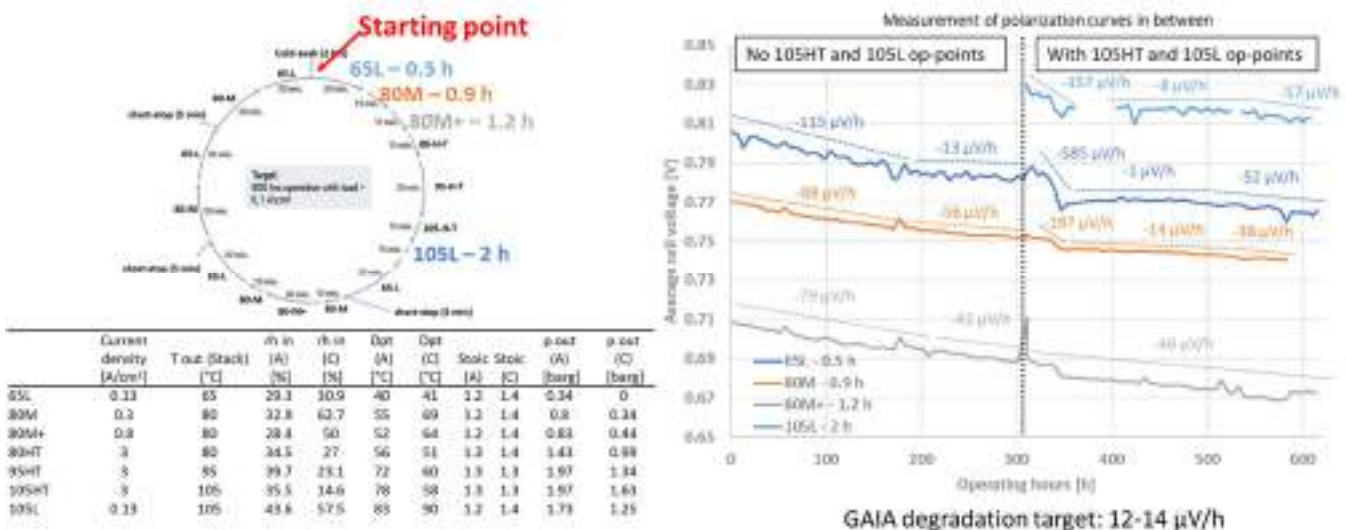


Figure 1: The drive cycle developed for GAIA fuel cell durability testing (top left, BMW) and a summary of the respective parameter sets of the operating points (bottom left, BMW). On the right, the evolution of the cell voltage over time of the first operating points of each drive cycle is demonstrated as an example for the operating points 65L, 80M, 80 M+ and 105L. Furthermore, the observed degradation rates of the operating points is displayed (ZSW data).

Furthermore, the performance of the stack drastically decreased with increasing operating time. This was indicated by a significant decay of the cell voltage of the measured polarisation curves when comparing the BoL and end-of-life (EoL) performance (Figure 2). Thereby, especially the mass transport properties but also the catalytic activity

decreased during the durability test. A further observation was the degradation of the membrane as sudden OCV drops beginning at operating hour 500 showed pinhole formation of the MEAs 4 and 8 (Figure 2).

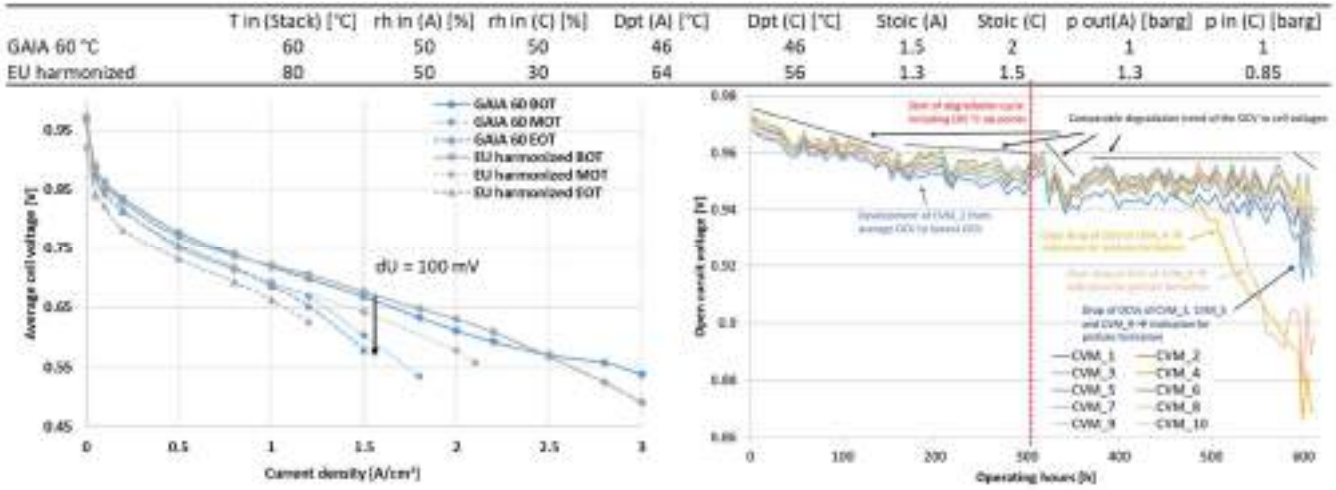


Figure 2: On the left side, the results of the polarisation curves measured at GAIA 60 and EU harmonised conditions (top) at the beginning (BOT), middle (MOT) and end of test (EOT) are demonstrated. On the right side, the open circuit voltage (OCV) over time is shown demonstrating a clear drop of cells 4 and 8 after 500 operating hours due to pinhole formation (ZSW data).

The Gen 2 short stack with an improved cathode catalyst carbon support and a GDL with improved mass transport properties demonstrated an even higher decay rate than Gen 1. The EoL performance at GAIA 60 conditions was comparable to that of the Gen 1 short stack (Figure 3). This was unexpected, as the Gen 2 stack had a significantly shorter operating time with only 250 hours, instead of the 1200 operating hours of the Gen1 stack.

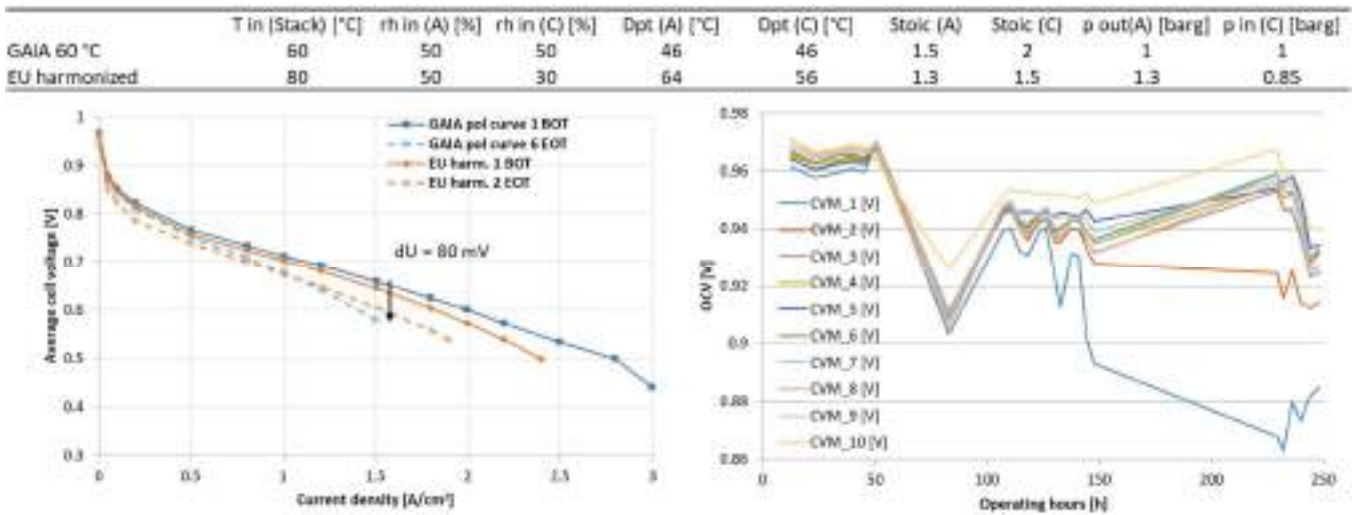


Figure 3: On the left side, the results of the polarisation curves measured at GAIA 60 and EU harmonised conditions (top) at the beginning (BOT) and end of test (EOT) are demonstrated. On the right side, the open circuit voltage (OCV) over time is shown demonstrating a clear drop of cells 1 and 2 at the end of test due to pinhole formation (ZSW data).

The observation of high decay rates during the Gen 1 and Gen 2 short stack testing were the basis for extensive post-mortem analyses. The goal of these analyses was to determine and eliminate the degradation mechanisms operating in these MEAs, for the Gen 3 and Gen 4 MEAs to successfully reach the GAIA durability target.

3. RESULTS AND DISCUSSION

During the GAIA project, various analytical methods were applied to determine the degradation mechanisms of the GAIA MEAs in post-test analysis. Therefore, post-test MEAs from small size single cells (50 cm²), automotive size single cells (285 cm²) and automotive size short stacks (285 cm², 4-10 cells) were analysed after performance or durability tests at BMW, JM, CNRS and ZSW test facilities. In order to complete the final stack testing within the period of the GAIA project, the possibility for material changes for the final MEA generation was limited up to the middle of 2021 to deliver the latest generation of MEAs in time. Therefore, only degradation mechanisms observed with post-test analyses of the first two MEA generations could be addressed by improving the materials used for the Gen 3 and Gen 4 MEAs. To date, no post-mortem analyses have been performed with the Gen 3 MEA since the material decision for the Gen 4 MEAs had to be made before the end of the Gen 3 stack test. Furthermore, no post-mortem analysis of the Gen 4 MEAs was carried out within the GAIA project, since the Gen 4 durability test was still on-going at the end of the GAIA project. Hence, this post-mortem analysis report focusses on the results of the post-mortem analyses performed with the stack generations Gen 1 and Gen 2. Table 1 shows an overview of the components of the four stack generations in the GAIA project as well as the non-scheduled generation 2 MEA Gen 2.1.

Table 1: Overview of the components of each GAIA stack generation. Post-mortem characterisation focussed on the stack generations Gen 1, Gen 2 and Gen 2.1.

| | Gen 1 | Gen 2 | Gen 2.1 | Gen 3 | Gen 4 |
|-------------------------------|---|---|---|---|---|
| Catalyst anode | JM benchmark cell reversal tolerance catalyst, 0.05 mgPt/cm ² – 0.043 mgIr/cm ² | JM benchmark cell reversal tolerance catalyst, 0.05 mgPt/cm ² – 0.043 mgIr/cm ² | JM benchmark cell reversal tolerance catalyst, 0.05 mgPt/cm ² – 0.043 mgIr/cm ² | JM benchmark cell reversal tolerance catalyst, 0.05 mgPt/cm ² – 0.043 mgIr/cm ² | JM benchmark cell reversal tolerance catalyst, 0.05 mgPt/cm ² – 0.043 mgIr/cm ² |
| Catalyst cathode | JM C2 benchmark catalyst, 0.4 mgPt/cm ² | JM C4 carbon support catalyst, 0.4 mgPt/cm ² | JM C4 carbon support catalyst, 0.4 mgPt/cm ² | JM C4 carbon support, Pt location control, 0.4 mgPt/cm ² | JM C4 carbon support, 0.25 wt% additive, 0.4 mgPt/cm ² |
| Ionomer catalyst layer | 3M XXXX EW |
| Membrane | JM V10i, thickness 15 µm | JM V10i, thickness 15 µm | Alternative ionomer 2, low basis weight PBI-X reinforced, thickness 13 µm | Alternative ionomer 1, ePTFE reinforced, thickness 10 µm | Alternative ionomer 2, low basis weight PBI-X reinforced, thickness 13 µm |
| GDL anode | H14CX653 | H14CX653 | H14CX653 | H14CX653 | H14CX653 |
| GDL cathode | H54CX653 | H54CX713 | H54CX713 | G54CX713 | G54CX713 |
| Test type | Performance + durability | Performance | Performance + durability | Performance + parameter optimization | Performance + durability |

Catalyst layer stability

In GAIA, the anode catalyst layer was unchanged during the MEA iterations. Hence, all MEA generations had the same anode thickness, loading, ionomer and catalyst. The cathode catalyst layer contained different types of catalyst but the same thickness, loading and ionomer (Table 1). One important point regarding the durability of an MEA is the stability of the catalyst layers, in particular the porous structure of the catalyst layer, the carbon support and the stability of the platinum particles. As demonstrated in figure 4, there was no observable difference regarding the morphology of the catalyst layers of the Gen 1 and Gen 2.1 MEAs. Both anode and cathode structure looked similar when comparing the high-resolution SEM images of the catalyst surfaces of the MEAs before and after testing. This means the porosity of the catalyst layers was maintained on a macroscopic level during fuel cell operation and no influence on the gas diffusion properties of the catalyst layer was expected.

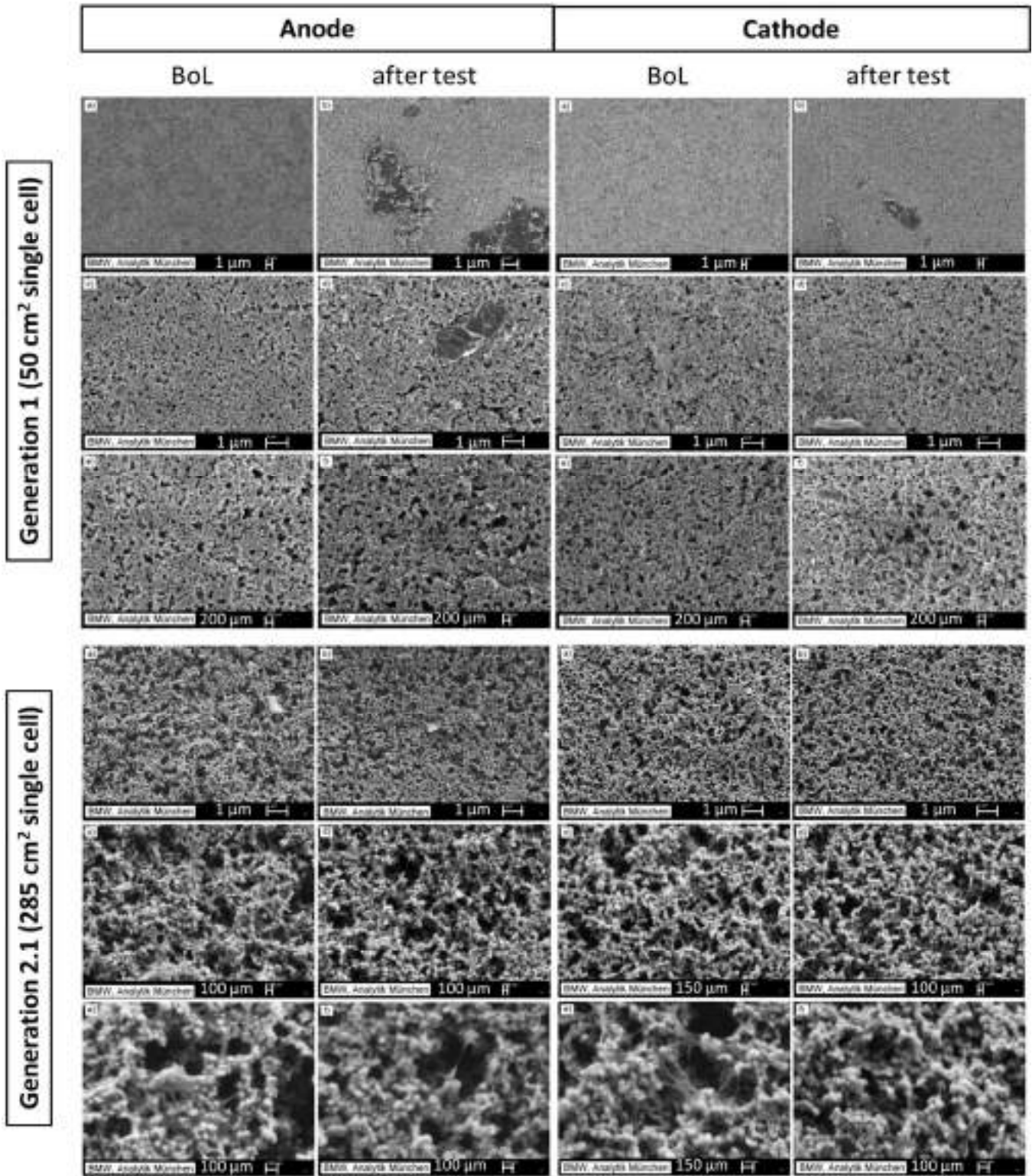


Figure 4: High-resolution SEM images from the catalyst layer surfaces of a Gen 1 (top) and a Gen 2.1 (bottom) at different magnifications. The catalyst layers before (column 1 and 3) and after (column 2 and 4) the test are displayed for the anode (column 1 and 2) and the cathode (column 3 and 4) (BMW data).

Figure 5 also demonstrates that there was no significant change in anode and cathode catalyst layer thickness for the investigated MEAs before and after the stack test. It is clearly visible that the anode catalyst layer had a constant thickness of approximately 5 μm whereas the cathode catalyst layer had a constant thickness of approximately 10 μm at all sample regions probed. This confirms the conclusion of no macroscopic changes of the catalyst layer structure previously made on the basis of the SEM images.

Table 2: Summary of results from different post-mortem characterisations made at JM comparing a pristine Gen 2.1 MEA with post-test Gen 2 and Gen 2.1 MEAs near the cathode inlet and outlet) (JM data). Column 1 shows the investigated parameter (JM data).

| Parameter | Control BOL Sample (Gen 2.1) | PBI Post Mortem Cathode Inlet (Gen 2.1, 285 cm ² single cell) | PBI Post Mortem Cathode Outlet (Gen 2.1, 285 cm ² single cell) | ePTE Post Mortem Cathode Outlet (Gen 2, 285 cm ² single cell) |
|---|------------------------------|--|---|--|
| EPSA [cm ² Pt/cm ²] | 170.1 | 167.8 | 158 | 56.4 |
| Knudsen Diffusion Resistance@68C [s/m] | 4 | 1.9 | 3 | 1.4 |
| Oxygen permeability diffusion resistance@68C [s/m] | 9.6 | 18.1 | 17.3 | 27.6 |
| Pressure dependent resistance @ 100kPa [s/m] | 47.8 | 52.3 | 50.9 | 60.0 |
| Catalyst Layer protonic Resistance (MS O) [Ωcm ²] | 0.49 | 0.652 | 0.601 | 0.686 |
| High Frequency Resistance (MS O) [Ωcm ²] | 0.104 | 0.093 | 0.106 | 0.274 |
| Catalyst Mass Activity [A/mgPt] | 0.081 | 0.084 | 0.047 | 0.009 |
| Catalyst Spec Activity [mA/cm ²] | 0.19 | 0.2 | 0.119 | 0.064 |

Besides the macroscopic structure of the catalyst layer, there are also degradation mechanisms taking place at the microscopic level. The preservation of the three-phase boundary at the catalyst particle/ionomer/gas phase interphase is crucial for the fuel cell performance. This interphase for instance degrades with a changing ionomer distribution, ionomer dissolution, Pt-particle agglomeration or Pt-dissolution. A reduction of the three-phase boundary lowers the area for the hydrogen oxidation or oxygen reduction reaction to take place and influences the fuel cell kinetics.

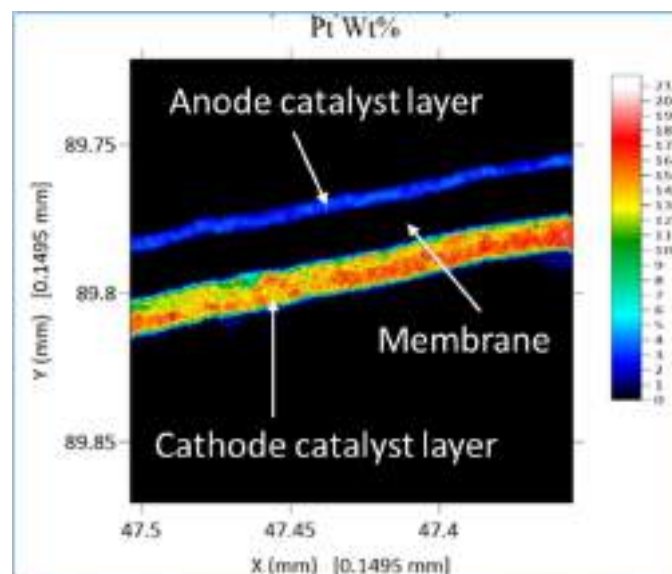


Figure 6: EPMA displaying the Pt-distribution of an MEA cross-section of the Gen 2.1 membrane after testing.

Looking at the cathode catalyst, there was a significant reduction of the active Pt surface area observed for the Gen 2 MEA indicated by a reduced EPSA (Electrochemical Pt Surface Activity) value after testing (Table 2). The reduction of the active Pt surface can be caused either by an agglomeration of the Pt particles or a dissolution of the Pt particles on the catalyst carbon support. Unfortunately, no further post-mortem analyses such as e.g., high-resolution cross-section SEM images, TEM-images, XRD or EDX measurements were made with the Gen 2 MEA to prove any of the degradation mechanisms for the reduction of the Pt active area.

In contrast, a stable active Pt area was observed by EPSA in case of the Gen 2.1 MEA. Additionally, no migration or dissolution of the Pt was observed by an MEA cross-section EPMA (Electron Probe Micro Analysis) as demonstrated in Figure 6. The Pt-distribution clearly demonstrated no Pt-band formation at the membrane and no Pt-particle agglomeration indicated by a still homogeneous Pt-distribution within the anode and cathode catalyst layers. The intactness of the cathode catalyst layers was also confirmed by the EDX mapping made at CNRS clearly demonstrating the Pt was still located exclusively in the catalyst layers. There was no Pt-band detected by EDX at the membrane surface (Figure 7).

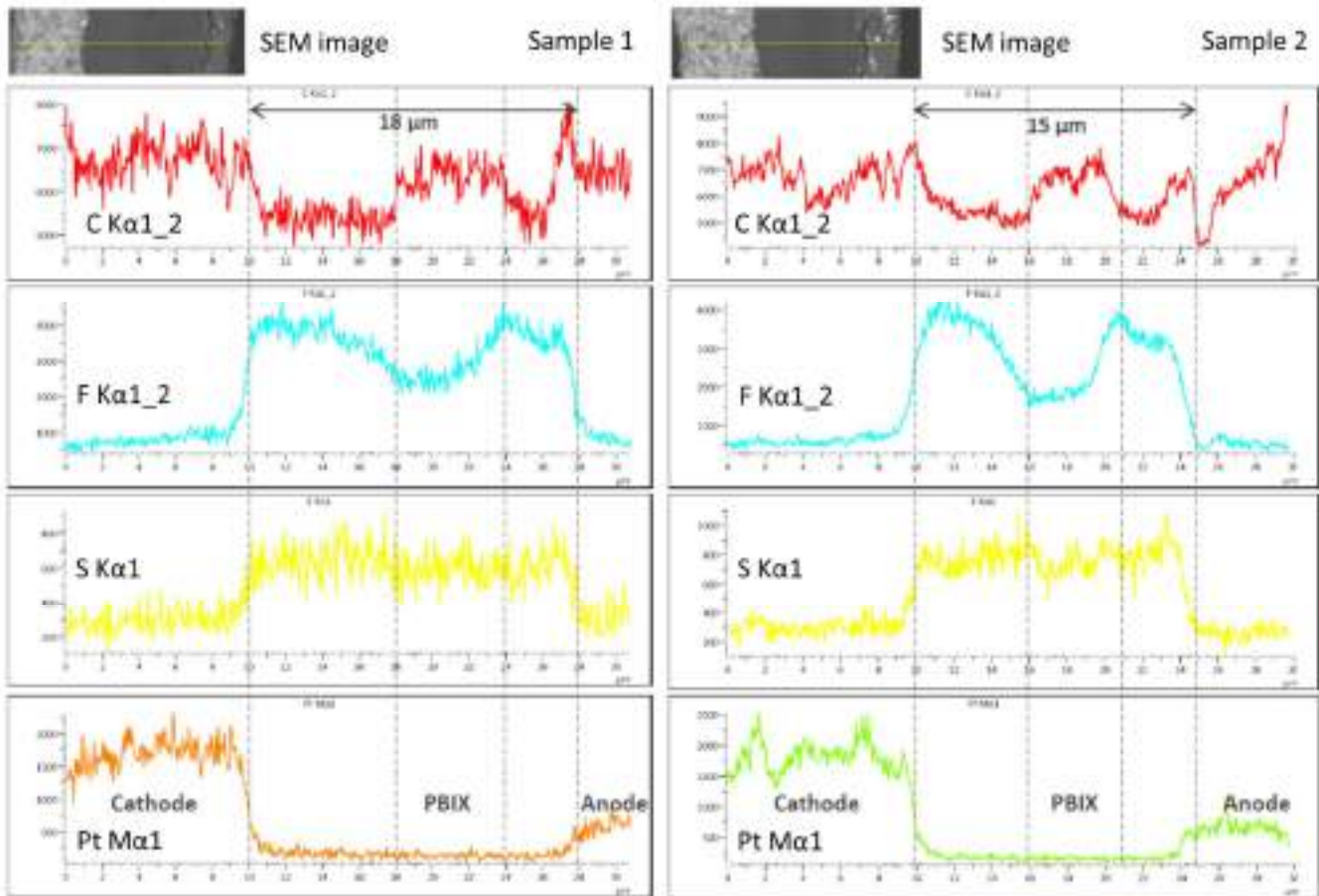


Figure 7: EDX mapping of two sample areas (left and right column) of the post-mortem Gen 2.1 MEAs showing the distribution of the elements carbon, fluorine, sulfur and platinum. On the y-axis the counts, on the x-axis the distance across the MEA cross-section (CNRS data).

Considering the ionomer stability of the catalyst layers, clear changes between the pristine and post-test MEAs were observed that affected the three-phase boundary and herewith the fuel cell performance decay. The parameters oxygen permeability resistance and catalyst layer protonic resistance drastically increased when comparing the pre- and post-test MEAs for both MEA types Gen 2 and Gen 2.1 (see Table 2). Thereby, the changes were even more pronounced for the Gen 2 MEA, which cannot be understood in detail, as the catalyst layers of Gen 2 and Gen 2.1 were identical. The oxygen permeability resistance is related to the ionomer distribution, which apparently decreased through ionomer migration or dissolution. The changes in protonic conductivity is related to a reduction of sulfonic groups, which indicated a loss of ionomer by ionomer dissolution. The dissolution of the ionomer was also detected when looking at SEM cross-section images, which clearly demonstrated migrated polymer fibres at the catalyst layers in cases of Gen 1, Gen 2 and Gen 2.1 post-test MEAs. This observation revealed a low stability of the ionomer used in the catalyst layer during the fuel cell operation at GAIA conditions.

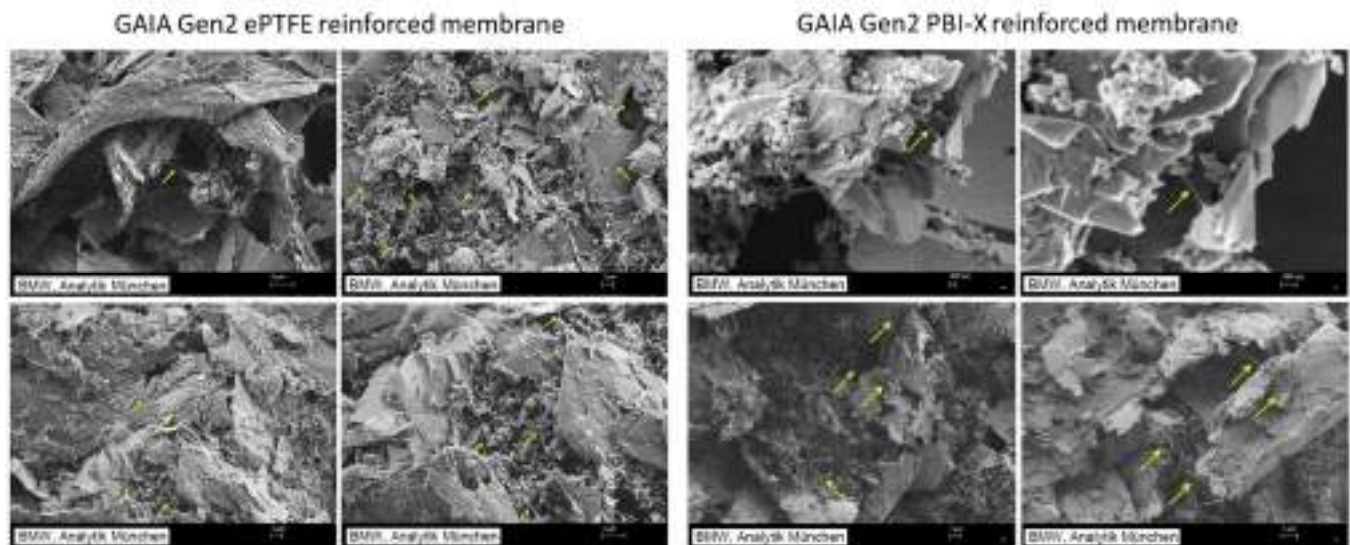


Figure 8: SEM images of the cathode MPL of a post-test Gen 2 (left) and Gen 2.1 (right) MEA. Four different areas are shown all indicating the presence of polymer fibres at the carbon particles marked by yellow arrows (BMW data).

There were two different assumptions made to explain the ionomer migration and dissolution in the catalyst layers. The first assumption was an increased aqueous solubility of the applied 3M 800 EW ionomer at the high operating temperature of up to 105 °C that would lead to washing out of the ionomer from the catalyst layer. The second assumption was ionomer chain breakage by free radical attacks, which would also increase the aqueous solubility of the shortened ionomer chains. The usage of ionomers with clearly higher molecular weight to increase the crystallinity and the usage of an additive suppressing the radical formation were discussed as possible solutions to decrease the ionomer dissolution and migration of the future MEAs significantly. Due to the short time frame in which to deliver the final MEA generations within the GAIA project duration, only the addition of a radical scavenger additive to the catalyst layer was implemented.

Membrane stability

To investigate the membrane stability, IR thermal imaging also known as thermography was performed with the post-test MEAs of the first stack generations Gen 1, Gen 2 and Gen 2.1. A gas flow consisting of 5 % dry hydrogen in dry nitrogen is supplied to the cathode side of the MEA, which is fixed within a special holder containing a flow field to guarantee a homogeneous gas distribution over the whole MEA area. If an MEA contains holes or thinner areas, the hydrogen reacts with the air passing through the weak spots of the MEA, which generates heat that is detected by an infrared camera.

On performing thermography with the Gen 1 post-mortem MEAs, clear hot spots with temperatures above 40 °C were detected for the cells 4 and 8 near the anode outlet area, which indicated pinhole formation (Figure 9). This observation fitted the electrochemical data that clearly demonstrated a drop of the open circuit voltage (OCV) of cells 4 and 8, which is a further indication for pinholes in the membrane. A hot spot at lower temperatures of 34 °C and smaller size indicated the beginning pinhole formation at cell 2, which also agrees with the beginning drop of the OCV during fuel cell testing.

Thermography with post-mortem Gen 2 MEAs from the 10-cells short stack also demonstrated clear pinholes in the cells with a pronounced OCV drop during the fuel cell testing (Figure 9). In particular, cell 1 demonstrated a large pinhole in the centre of the MEA, whereas cell 2 indicated a starting pinhole formation near the anode outlet area. The trend to pinholes near the anode outlet area was assumed to be related to local hydrogen starvation events leading to carbon oxidation of the polymer membrane. This progressively reduced the thickness of the membrane with increasing operating hours until pinholes formed. The large pinhole formed at the centre of MEA 1 was probably caused by a defect spot at the pristine MEA as it appeared at an early test stage and is not located within the typical area near the anode outlet.

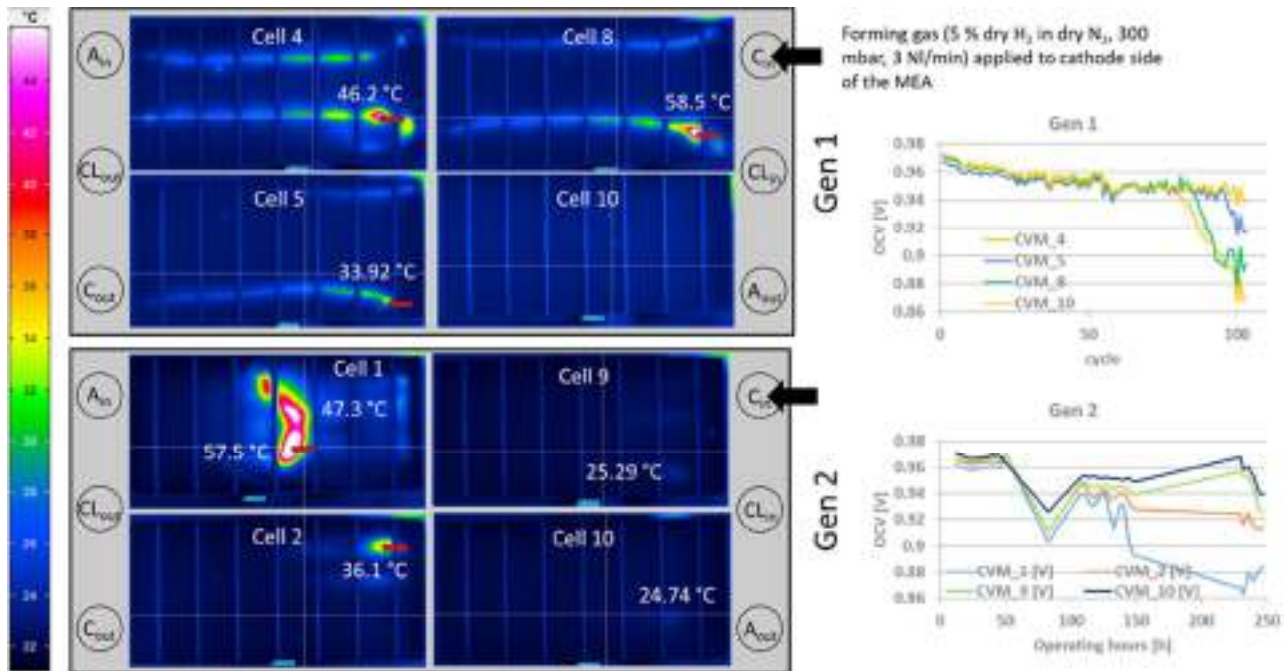


Figure 9: Left: Results of the thermographic analysis of post-mortem MEAs from the Gen 1 (top) and Gen 2 (bottom) short stack. Right: OCV development of the four investigated post-mortem MEAs from the Gen 1 and Gen 2 short stacks (ZSW data).

The optical microscopy images recorded on cross-sections prepared from the Gen 2 post-mortem MEAs confirmed the assumption of an insufficient membrane stability of the ePTFE reinforced membranes. Figure 5 clearly demonstrates a much thinner membrane of the aged Gen 2 samples of only 6 μm in comparison to the initial 15 μm of the pristine Gen 2 MEA. Thereby, it is remarkable that the thinning is completely limited to the membrane while both catalyst layers still maintained their initial layer thickness.

In contrast to the Gen 2 MEA with ePTFE reinforcement, the effect of the membrane thinning was not observed with the PBI-X reinforced Gen 2.1 MEA. The microscope images (Figure 5) of the cross-sections prepared demonstrated the same membrane thickness of the membrane before and after single cell long-term testing. This observation was also confirmed by post-test thermography imaging of Gen 2 and Gen 2.1 MEAs (Figure 10). It is clearly visible that there was no indication of pinhole formation detected in case of the PBI-X reinforced membrane, whereas the ePTFE reinforced Gen 2 MEA demonstrated clear pinhole formation especially near the anode outlet region again. Based on this finding, PBI-X was used as the membrane reinforcement for the Gen 4 MEAs as it increased the membrane stability significantly.

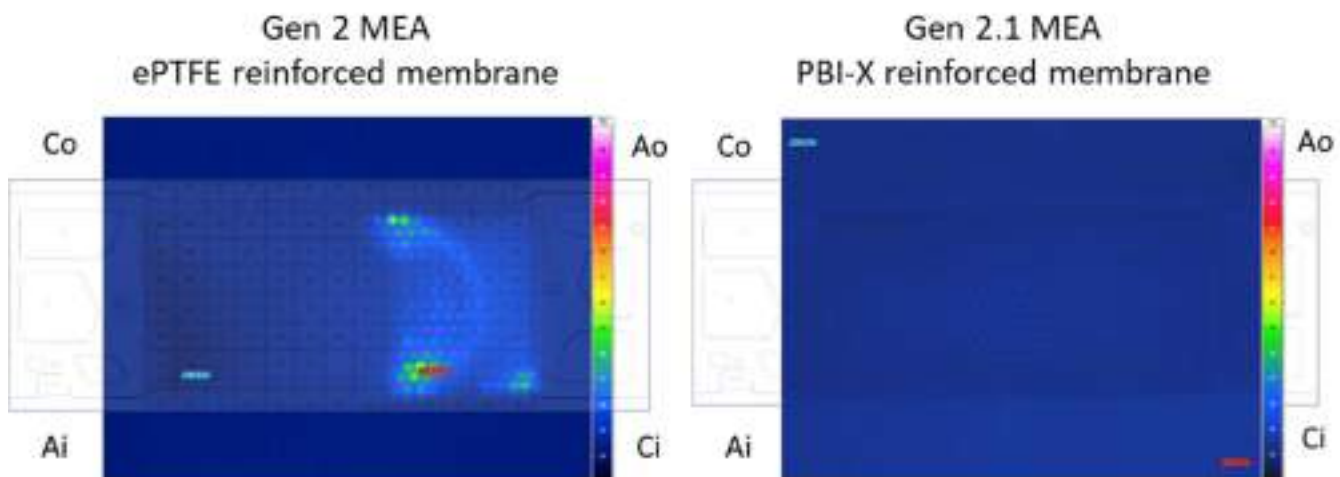


Figure 10: Thermography images comparing the ePTFE reinforced Gen 2 MEA (left) with the PBI-X reinforced Gen 2.1 MEA (right) after long-term testing (BMW data).

Gas diffusion layer stability

To investigate any changes in the hydrophobicity of the GDL substrate, the sessile drop method was used to determine the contact angles of post-mortem MEAs from the Gen 1 and Gen 2 short stacks. Therefore, two rows of eight droplets each with a distancing of 1 cm were measured for nine different sectors of the GDL surface (Figure 11). Thereby, the measured contact angles for each row of eight droplets were averaged giving two values for each of the nine investigated GDL surface areas. The calculated, relatively high, error of the contact angles corresponded to the method itself and even more to the quite pronounced surface inhomogeneity of the investigated GDL substrates.

The comparison of the measured contact angles of the pristine and the post-mortem GDL revealed a clear decrease of the hydrophobicity of the GDL substrates for Gen 1. This observation was related to a dissolution of the hydrophobic agent PTFE at the high current density and temperature.

Furthermore, there was a difference of hydrophobicity loss detected for the anode and cathode GDL. The hydrophobicity of the anode GDL (-9.1 °) decreased less than the hydrophobicity of the cathode GDL (-15.8 °). Looking at the contact angles from the different surface sections, the anode GDL substrate demonstrated a slightly lower heterogeneity compared to the cathode GDL substrate. Finally, the cathode GDL hydrophobicity revealed a trend towards lower values near the anode outlet area.



Figure 11: Results of the contact angle measurement of the Gen 1 post-test MEAs. The contact angles of 18 lines of eight droplets each from nine different MEA region. On top, the results measured for the anode GDL, on bottom the results measured for the cathode GDL. There were five different post-test MEAs analysed. The colour code is related to measured contact angles with high values marked in green going to low values marked in red.

The same trends as observed with the post-test GDL substrates from the Gen 1 stack were present in case of the Gen 2 post-test GDL substrates. Figure 12 demonstrates a map of contact angle differences of the pristine and the post-test GDL substrates for one exemplary Gen 1 and Gen 2 MEA. The contact angle difference of the anode GDL is displayed in blue, whereas the contact angle difference of the cathode GDL is displayed in red. Thereby, the degradation of the hydrophobicity is similar for both generations with around -9 °, while the Gen 1 cathode was an exception with -15.8 °. The difference might be explained by the much longer test duration of the Gen 1 stack, which likely follows different ageing mechanisms. The trend towards a larger decrease of the hydrophobicity near the anode outlet area was observed for the Gen 1 cathode, Gen 2 anode and Gen 2 cathode. The mechanisms behind the hydrophobicity loss remained unknown.

One remarkable finding was the fact, that in areas with pinhole formation, the degradation of the cathode GDL hydrophobicity was significantly higher than in other areas. This fact was observed for the Gen 1 and Gen 2 post-mortem MEAs as demonstrated in Figure 12. One explanation would be the oxidation of the carbon compounds of the GDL substrates due to the kind of “internal combustion” at the pinholes. Thereby, the pinholes represent a spot where the catalytic reaction of hydrogen and oxygen can take place directly creating a reactive zone. This zone contains free radicals that also attack the GDL substrate.

The reduction of the hydrophobicity of the GDL substrate influences the water management of the fuel cell during operation. Nevertheless, the influence on the MEA degradation was considered to be rather low. Hence, no efforts were made within the GAIA project to improve the stability of the hydrophobic properties of the GDL.

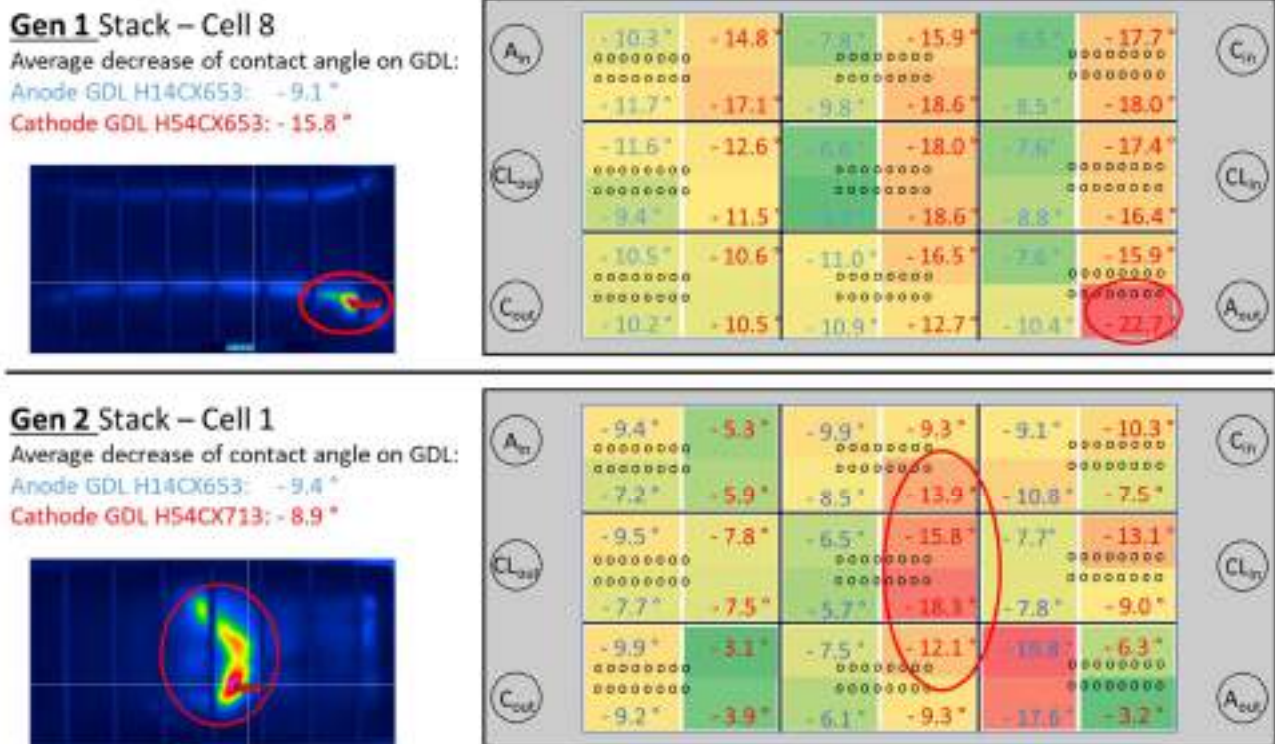


Figure 12: Locally resolved changes of the contact angles of the anode (blue) and cathode (red) GDL of the MEA 8 from the Gen 1 stack (top) and the MEA 1 from the Gen 2 stack (bottom). The circles represent to locations of the droplets used for contact angle measurement on the GDL surface.

4. CONCLUSIONS AND FUTURE WORK

A comprehensive set of post-mortem analyses of the first two MEA generations of the GAIA project revealed two major reasons for the observed MEA degradation. The first reason was an insufficient stability of the ionomer applied within the catalyst layers at the GAIA operating conditions at high current density of 3 A/cm² and high temperature up to 105 °C. Thereby, a significant amount of catalyst layer ionomer migrated or was dissolved during fuel cell operation leading to a clear increase of the oxygen diffusion and protonic conductivity of the catalyst layers. To overcome this problem, a radical scavenging additive was added to the final MEA generation Gen 4 to mitigate free radical attack on the catalyst layer ionomer.

The second reason for the increased stack degradation of the first stack generations was low membrane stability, which yielded into pinhole formation of the ePTFE reinforced membranes after just a moderate time of operation. In contrast, a PBI-X reinforced MEA derivative of the Gen 2 MEA did not show any indication of pinhole formation after a modified durability test without high temperature operation and high current density, since the membrane showed still the same thickness as the pristine sample and not a single pinhole during the thermography measurements. Hence, the PBI-X reinforced membrane was used in the Gen 4 MEA to reach the GAIA durability target. Furthermore, an adjustment of the operating parameters including an increase of the hydrogen stoichiometry was decided upon, to avoid pinhole formation due to hydrogen starvation events. With the PBI-X reinforced membrane and adjusted operating parameters, the Gen 4 MEA demonstrated a clearly increased



This project has received funding from the Fuel Cells and Hydrogen 2 Joint Undertaking (now Clean Hydrogen Partnership) under grant agreement n°826097. This Joint Undertaking receives support from the European Union's Horizon 2020 Research and Innovation program, Hydrogen Europe and Hydrogen Europe Research.



stability especially at high temperature operation and high current density (see Deliverable 6.3). The observed OCV degradation of approximately $-10 \mu\text{V/h}$ during the first 600 operating hours was absolutely within the target and never reached with the previous membrane generations. Nevertheless, after 600 operating hours, the harsh operating conditions induced pinhole formation yielding into an increased stack degradation. Post-mortem analysis of the Gen 4 MEAs outside the time frame of the GAIA project are going to be used to determine the reasons for the observed membrane degradation after 600 operating hours.